The Enthalpy of Acyl Chain Packing and the Apparent Water–Accessible Apolar Surface Area of Phospholipids

ARTICLE *in* BIOPHYSICAL JOURNAL · FEBRUARY 2001

Impact Factor: 3.97 · DOI: 10.1016/S0006-3495(01)76012-2 · Source: PubMed

The Enthalpy of Acyl Chain Packing and the Apparent Water-Accessible Apolar Surface Area of Phospholipids

Heiko Heerklotz and Richard M. Epand
Department of Biochemistry, Health Sciences Centre, McMaster University, Hamilton, Ontario, Canada

ABSTRACT The energetics of phospholipid aggregation depend on the apparent water-accessible apolar surface area (ASA_{ap}), ordering effects of the chains, and headgroup interactions. We quantify the enthalpy and entropy of these interactions separately. For that purpose, the thermodynamics of micelle formation of lysophosphatidylcholines (LPCs, chains C_{10}, C_{12}, C_{14}, and C_{16}) and diacylphosphatidylcholines (DAPCs, chains C_5, C_6, and C_7) are studied using isothermal titration calorimetry. The critical micelle concentration (CMC) values are 90, 15, and 1.9 mM (C_5–C_7-DAPC) and 6.8, 0.71, 0.045, and 0.005 mM (LPCs). The group contributions per methylene of $\Delta\Delta G^0 = -3.1$ kJ/mol and $\Delta\Delta C_P = -57$ J/(mol · K) for LPCs agree with literature data on hydrocarbons and amphiphiles. An apparent deviation of DAPCs (−2.5 kJ/mol, 45 J/(mol · K)) is due to an intramolecular interaction between the two chains, burying 20% of the surface. The chain/chain interaction enthalpies in a micelle core are by ~−2 kJ/(mol) per methylene group more favorable than in bulk hydrocarbons. We conclude that the impact of the chain conformation and packing on the interaction enthalpy is very pronounced. It serves to explain a variety of effects reported on membrane binding. Interactions within the water-accessible region show considerable ΔH, but almost no ΔG^0. The heat capacity changes suggest about three methylene groups ($ASA_{ap} \approx 100$ Å^2) per LPC remain exposed to water in a micelle (DAPC: 2 CH_2/70 Å^2).

INTRODUCTION

In this study we address a number of important issues for biomembrane function by thermodynamic means. What is the water-accessible apolar surface area per phospholipid and how much energy is associated with the formation? To what extent do lipid acyl chains resemble the behavior of bulk hydrocarbons? Are chain/chain interactions sensitive to changes in packing in the membrane? What accounts for the enthalpies of binding of solutes into lipid membranes?

The self-assembly of lipids, proteins, and other membrane constituents is driven by the hydrophobic effect. Hence, changes of the apparent water-accessible apolar surface (ASA_{ap}) control the energetic costs for expanding a lipid membrane. Such a lateral expansion may occur upon insertion of antibiotic or fusion peptides (Ludtke et al., 1995) or be required to match the hydrophobic thickness of membrane proteins, which can proceed via gradual demixing of lipids with different chain lengths and/or by a disordering of the chains (Killian, 1998). It will, furthermore, be related to the probability of effects such as head/tail contacts (Huster et al., 1999) and molecular protrusions (Israelachvili and Wennerstrom, 1996). However, the ASA_{ap} of lipids is not known and cannot simply be assessed from structure information because the effects of the rough geometry of the interface and the proximity of the headgroups, particularly on the thermodynamic properties of interfacial water, are not clear. Here we pursue a thermodynamic approach to estimate this important quantity. It is based on the fact that ASA_{ap} is directly related to the isobaric heat capacity, C_p (cf. Kresheck and Hargraves, 1974; Gill and Wadsö, 1976; Sharp and Madan, 1997). In fact, the concept of the solvent accessible surface area has been developed to quantitatively predict protein/ligand interactions (Baker and Murphy, 1998) or protein folding properties (Spolar et al., 1992). Blume (1983) measured absolute values of C_p for phospholipids by means of differential scanning calorimetry. Although it is not straightforward to separate contributions from different moieties to the overall C_p, this study revealed that "more water than previously estimated may be present in the hydrophobic interior of the membrane." We measure the enthalpy change upon transfer between the aqueous phase and the lipid aggregate as a function of temperature. This yields the heat capacity difference between the two states (ΔC_p) rather than absolute C_p values. It can be achieved by means of isothermal titration calorimetry and has the advantage that all contributions to C_p that remain unchanged upon aggregation are excluded, and one can essentially focus on hydrophobic interactions (Kresheck and Hargraves, 1974; Kresheck, 1998; Paula et al., 1995). However, this technique requires a sufficient water solubility of the molecules and, thus, prohibits application to long-chain, bilayer-forming phospholipids. We have therefore studied short-chain diacylphosphatidylcholines (DAPCs) and lysophosphatidylcholines (LPCs). Whereas LPCs form spherical micelles, the investigated DAPCs associate to spherical (C_5-DAPC), ellipsoidal (C_6-DAPC), and rod-like (C_7-DAPC) micelles (Eastoe et al., 1998).

Another goal of the current work is to quantify the thermodynamic effects of the ordering of the hydrocarbon chains in an aggregate. Phillips et al. have already stressed in 1969 that liquid crystalline acyl chains have intermediate thermodynamic properties between solids and liquids. Nev-

Received for publication 10 January 2000 and in final form 18 October 2000.

Address reprint requests to Dr. Heiko H. Heerklotz, Dept. of Biophysical Chemistry, Biocenter of the University of Basel, Klingelbergstrasse 70, CH-4056 Basel, Switzerland. Tel.: 41-61-2672192; Fax: 41-61-2672189; E-mail: heiko.heerklotz@unibas.ch.

0006-3495/01/01/271/09 $2.00

ertheless, the thermodynamics of the hydrophobic core of micelles or membranes have mostly been approximated by those of liquid hydrocarbon. Consequently, enthalpies of association measured at room temperature, where changes in hydrocarbon/water contacts yield no heat, have been assigned to headgroup interactions. Recently, DeVido et al. (1998) have studied hydrocarbon chains attached to a solid surface, demonstrating that aligned chains may exhibit a substantially different thermodynamic behavior than amorphous liquids. Their subject differed from the situation in a bilayer by the fact that the surface density of the chains was fixed and could not relax to the optimum value. Here we directly quantify the chain/chain interaction enthalpies in a liquid crystalline phase. The considerable effects obtained have important consequences for the partitioning of molecules into membranes. They can also be considered a quantitative basis for understanding the anomalous, exothermic heat of binding of peptides to small lipid vesicles, which has been established as the nonclassical hydrophobic effect by Seelig and Ganz (1991).

Beside constituting model systems for membrane lipids, these substances themselves have important biological functions. For example, small concentrations of LPCs regulate a broad range of cell processes (Yuan et al., 1996) and inhibit membrane fusion (Kluge et al., 1987; Chernomordik, 1996). Short-chain DAPCs have been identified as superior "detergents" for the solubilization and functional reconstitution of membrane proteins (Kessi et al., 1994). Furthermore, they have been used to form bicelles, membrane models that can be oriented in a magnetic field (Sanders and Landis, 1995; Vold and Prosser, 1996).

The well-known ITC demicellization protocol was used for measuring systems with CMC values between 5 μM and 16 mM. This protocol is based on injections of a micellar solution at ~20 times the CMC into buffer (Olofsson, 1985; Paula et al., 1995). It fails in the case of systems with a CMC in the 100 mM region. To include divaleroyl-PC, we establish a novel ITC technique.

MATERIALS AND METHODS

Materials

The substances were purchased from Avanti Polar Lipids, Alabaster, AL, and used without further purification. In the text, we will denote the one-chain, lysolipids as C_{10}-LPC (1-capryl-2-hydroxy-*sn*-glycero-3-phosphocholine), C_{12}-LPC (1-lauroyl-2-hydroxy-*sn*-glycero-3-phosphocholine), C_{14}-LPC (1-myristoyl-2-hydroxy-*sn*-glycero-3-phosphocholine), and C_{16}-LPC (1-palmitoyl-2-hydroxy-*sn*-glycero-3-phosphocholine). The diacylphospholipids are referred to as follows: C_5-DAPC (1,2-divaleroyl-*sn*-glycero-3-phosphocholine), C_6-DAPC (1,2-dicaproyl-*sn*-glycero-3-phosphocholine), and C_7-DAPC (1,2-diheptanoyl-*sn*-glycero-3-phosphocholine). The substances were dissolved in 20 mM Pipes buffer, at pH 7.4, containing 1 mM EDTA and 150 mM NaCl. Experiments performed with pure water for C_{10}-LPC and C_{12}-LPC showed no significant difference from the experiments performed with buffer. The calorimetric experiments were carried out on isothermal titration calorimeters (Omega and VP) produced by MicroCal, Northampton, MA.

ITC demicellization experiment

This protocol has been explained in detail elsewhere (Olofsson, 1985; Heerklotz et al., 1996; Paula et al., 1995; Kresheck, 1998). Briefly, the injection syringe is filled with a micellar dispersion and the cell is filled with buffer. The injectant concentration has to be chosen in order to reach about twice the CMC in the cell after the titration, i.e., at ~20 times the CMC for a 150 μl syringe and the 1.3 ml cell. The heat power peaks after each injection (cf. Fig. 1 *A*) are integrated versus time from the baseline and normalized with respect to the number of moles of titrant injected, yielding the observed heat in kJ/(mol injected), q_{obs}.

This quantity is plotted versus the average value of the surfactant concentrations in the cell before and after the respective injection (cf. Fig. 1 *B*). The plots exhibit the typical sigmoidal behavior with the heat of disintegration of the injected micelles vanishing when the CMC is reached in the cell. Some confusion arises from the fact that the CMC constitutes a broad range rather than a sharp transition described by simple models. From a thermodynamic point of view, it is most reasonable to define the point of inflexion of the sigmoidal curve, i.e., the maximum of the first derivative (cf. Fig. 1 *C*) as the CMC.

Different definitions have also been used for the enthalpy of micelle formation, ΔH, because a systematic trend of the titration heat may appear below the CMC due to intermolecular interactions between monomers. Our ΔH data refer to the state of dilute molecules compared to that of dilute micelles. That means the heat of demicellization is determined by subtracting the heat measured above the CMC from the heat extrapolated to vanishing surfactant concentration. The enthalpy of micelle formation differs only in sign from the enthalpy of demicellization. Note that the heat in Fig. 1 *B* is normalised with respect to the total lipid injected, $c^{syr} \cdot \Delta V$, calculated from the lipid molar concentration in the syringe, c^{syr}, and the injection volume ΔV. In fact, only the micellar part of the injectant, $(c^{syr}\text{-cmc}) \cdot \Delta V$, gives rise to a demicellization heat. Therefore, the ΔH data read from the plot were corrected by the factor $c^{syr}/(c^{syr}\text{-cmc})$.

Alternative ITC protocol for high-CMC substances

The demicellization protocol discussed above reaches its limit for substances with a very high CMC, such as C_5-DAPC. A syringe concentration of 20 times the CMC, as is the rule for the demicellization protocol using a 150 μl syringe and 1.3 ml cell, amounts to 1.8 M for C_5-DAPC (CMC = 90 mM). Such a high concentration has two major disadvantages. First, it may give rise to large intermicellar interactions that deviate considerably from the model approximations. Second, a large amount of material is required. The protocol described below does not require concentrations higher than 1.5–2 times the CMC. Whereas the protocol described in the previous section checks the cell content for the existence of micelles, the alternative approach detects micelles in the syringe. For that purpose, a set of experiments is performed with surfactant dispersions of varying concentration filled into the syringe. Each experiment requires only a single, small injection into buffer (practically, five injections are done and averaged). If the syringe contains no micelles, no heat of demicellization will be measured. The quasi-infinite dilution might, however, yield some heat of dilution we refer to as Q_{dil}^{mon}, which is supposed to be small but may vary somewhat with temperature and monomer concentration in the syringe, c^{syr} (sub-CMC behavior):

$$\frac{q}{\Delta V} = Q_{dil}^{mon}(c^{syr}) \qquad (1a)$$

If the concentration in the syringe, c^{syr}, is above the CMC, the volume of the injection, ΔV, contains $\text{CMC} \cdot \Delta V$ moles of monomers and $(c^{syr}\text{-CMC}) \cdot \Delta V$ moles of surfactant localized in micelles. Upon infinite dilution, the monomer fraction yields a constant heat Q_{dil}^{mon} (CMC). The micellar fraction gives rise to the heat of demicellization, $-\Delta H$ (note that ΔH refers to

micelle formation), yielding for the above-CMC behavior:

$$\frac{q}{\Delta V} = -(c^{\mathrm{syr}} - \mathrm{CMC}) \cdot \Delta H + Q_{\mathrm{dil}}^{\mathrm{mon}}(\mathrm{CMC}) \qquad (1b)$$

This equation predicts a linear relationship of the absolute heat per injection volume, $q/\Delta V$, versus the syringe concentration, c^{syr}, with a slope of $-\Delta H$. The concentration at the onset of a linear behavior indicates the CMC. Note that the syringe needs to be completely filled, which requires ~400 μl. We have performed five injections of 3 μl each (all representing quasi-infinite dilution), and measured at three temperatures. That means only 45 μl of the syringe content are actually used. To save material, we have started with the highest intended c^{syr} and have successively diluted the remaining dead volume sample to prepare the subsequent syringe contents.

RESULTS

Critical micelle concentration

Typical plots for the "classic" demicellization protocol are shown in Fig. 1. The curves indicate a very gradual process of micellization as a function of the lipid concentration. This is the typical behavior that has been shown for a large number of different surfactants already (for example, cf. Olofsson, 1985; Heerklotz et al., 1996; Paula et al., 1995; Kresheck, 1998). It is in conflict with the phase model of micelle formation, which would suggest a sharp transition as well as being against the mass action model, which implies a highly cooperative behavior for realistic aggregation numbers (e.g., 58 for C_6-DAPC, 120 for C_7-DAPC (Eastoe et al., 1998)). A quantitative description of the transition has been published for cholates (Paula et al., 1995), which form very small aggregates. Other surfactants appear to form intermediate structures (with intermediate chemical potentials) close to the CMC, and the fact that nothing is known about the molar enthalpy in these intermediates makes a quantitative modeling of the demicellization curve difficult. Nevertheless, the CMC is an important and useful quantity even though the association process cannot be accurately described as a transition between two states at a critical concentration. Its determination does require an empirical definition. It turns out that different CMC measurements determine, in fact, different quantities. Hydrophobic dyes that are quenched by water (e.g., pyrene) detect the occurrence of first aggregates, whereas a constant surface tension indicates that the transition is essentially completed and the monomer concentration remains constant. The concentration of maximum progress of association, which is approximated by the point of inflection (Kresheck, 1998) or, equivalently, the maximum of the first derivative (Paula et al., 1995) of the sigmoidal ITC curves has been found superior for a thermodynamic discussion. This value is given in Table 1 and plotted versus the chain length in Fig. 3.

The data obtained for D_5-DAPC by the alternative protocol described in the previous section are displayed in Fig. 2. The traces exhibit the behavior expected from the theoretical discussion. The heat measured at low titrant concentrations (well below the CMC) is rather small and only slightly concentration-dependent. Beyond ~100 mM, the exothermic heat of injection starts to grow linearly with the titrant, indicating that the CMC has been reached. The slope of these $q/\Delta V$ vs. C_D lines (Fig 2) yields ΔH according to Eq. 1. We have estimated the CMC as the point of intersection between lines describing the sub-CMC and the above-CMC data. All data are consistent with the thermodynamic requirement that the minimum CMC occurs at the isocaloric temperature (see below).

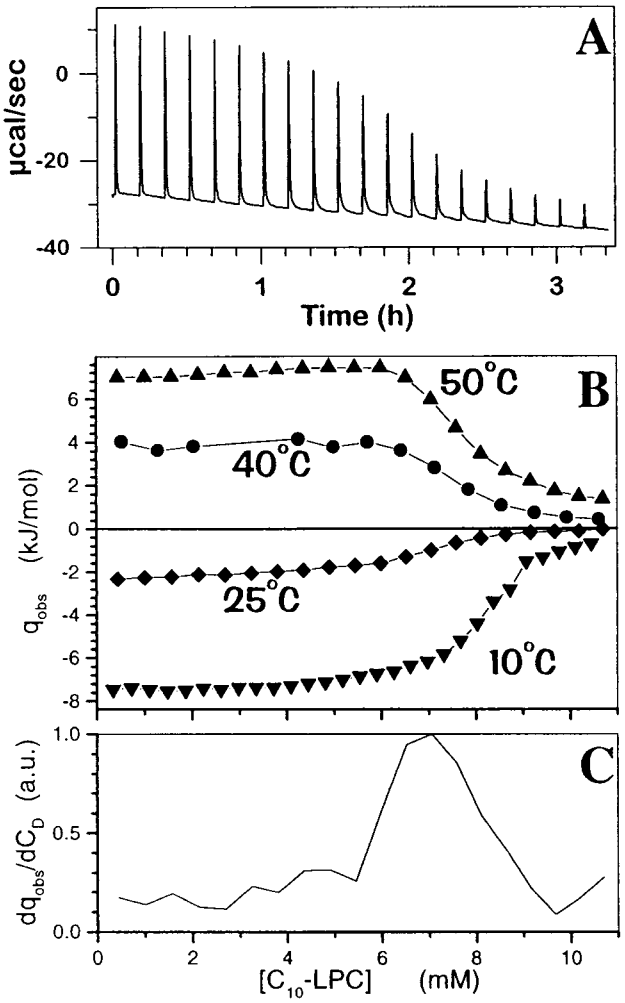

FIGURE 1 (*A*) Raw data of an ITC demicellization experiment. A 100 mM solution of C_{10}-LPC was injected in 20 increments of 7.5 μl each into the cell (1.3 ml) initially filled with buffer, at 50°C. The plot displays the heat power consumed in the cell (endothermic) versus experimental time. (*B*) Integrated and normalized heat, q_{obs}, of the experiment shown in *A* (and repetitions at other temperatures as specified in the plot) versus lipid concentration. The sigmoidal transition represents the appearance of micelles in the cell. (*C*) The progress of the transition at 25°C obtained as the first derivative of the trace in *B*. The maximum is referred to as the CMC.

Enthalpies of micelle formation

The enthalpies of micelle formation, ΔH, are given in Table 1 and are plotted versus temperature, *T*, for all compounds

TABLE 1 The enthalpy of micelle formation, ΔH, and the critical micelle concentration, CMC, measured by means of ITC demicellization experiments at different temperatures T

	T (°C)	ΔH (kJ/mol)	CMC (mM)
C_{10}-LPC	11.4*	7.6	8.2
	12.7	7.3	7.4
	25.0*	2.7	6.8
	40.4*	−4.0	7.1
	49.2	−6.7	7.4
	50.1*	−6.3	7.2
C_{12}-LPC	7.8	7.4	0.74
	7.5*	7.5	0.76
	25.1*	−0.5	0.74
	25.1	−0.7	0.68
	40.1*	−7.0	0.78
	50.1*	−13.8	0.90
	50.2	−12.6	0.86
C_{14}-LPC	7.4	5.7	0.045
	11.4	3.9	0.045
	19.9	−1.3	0.045
	30	−7.5	0.050
	40.5	−14.8	0.065
	50.4	−19.5	0.075
C_{16}-LPC	4	6.4	0.007
	10	2.1	0.005
	26	−8.4	0.005
	28	−15.9†	0.006
	35	−8.5†	0.006
	49	−15.4†	0.010
	49	−18.4†	0.008
	70	−7.0†	0.015
C_5-DAPC	10	13.3	105
	25	8.7	90
	40	4.9	85
C_6-DAPC	10.7	12.4	15
	24.8	6.5	16
	24.9	6.7	15
	38.1	1.5	15
	50	−2.7	16
C_7-DAPC	9.6	9.5	2.1
	25.2	2.3	1.9
	50.7	−9.2	2.1

Errors are typically ±0.4 kJ/mol for ΔH and ±10% for CMC; individual error bars are displayed in Figs. 3 and 4, and are considered in the fit procedures.

* Measured in water.

† Measurements might suffer from artifacts and have not been considered in discussion.

shown in Fig. 4. All data (except C_{16}-LPC, see below) are consistent with a linear relationship between ΔH and the temperature, T. Linear fits were done according to

$$\Delta H = \Delta C_p \cdot (T - T^*) \quad (2)$$

where the slope equals the change in isobaric heat capacity, ΔC_p, and the point of intersection with the abscissa is referred to as the isocaloric temperature, T^*. The results are given in Table 2. With increasing chain length, the isocaloric temperature decreases and ΔC_p becomes more negative.

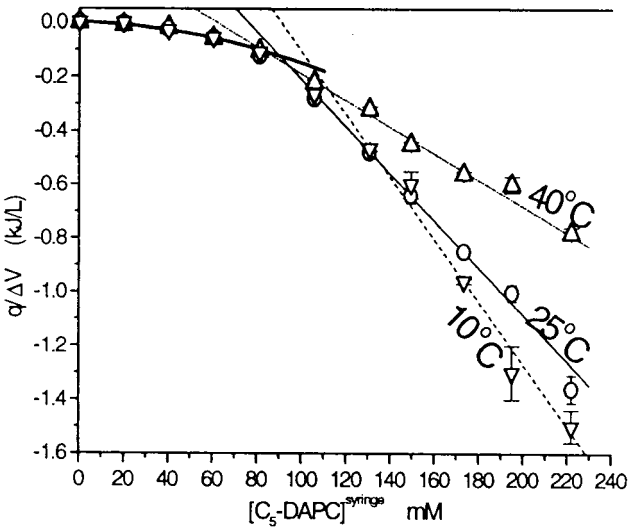

FIGURE 2 The heat of "infinite" dilution of dispersions of C_5-DAPC of different concentration (abscissa) into buffer, given in kJ/l injected (injection volume 3 μl). The experiments were performed at 10°C (▽), 25°C (○), and 40°C (△). The heat of monomer dilution measured up to the CMC of ~100 ± 20 mM appears to be basically independent of temperature. The slopes beyond the CMC, which are equal to the heat of micelle dissociation to isolated monomers, are listed in Table 1.

The data measured for C_{16}-LPC are compatible with a linear $\Delta H(T)$ behavior only at $T \leq 26$°C (cf. Table 1, Fig 4.). One might expect a phenomenon such as a cloud point to be responsible for that, but the detailed clarification of the effect is beyond the scope of this paper. For an estimate of ΔC_p and the determination of T^* and ΔH(23°C) we have only considered experiments up to 26°C (cf. Fig 4, Table 2).

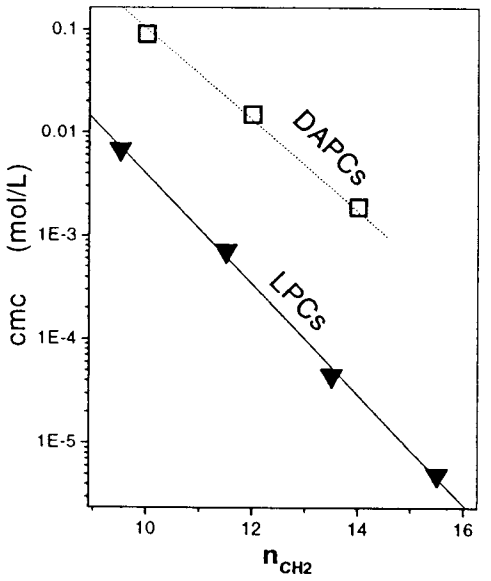

FIGURE 3 The critical micelle concentrations of DAPCs (□) and LPCs (▼) versus total number of methylene groups in their chains (n_{CH2}).

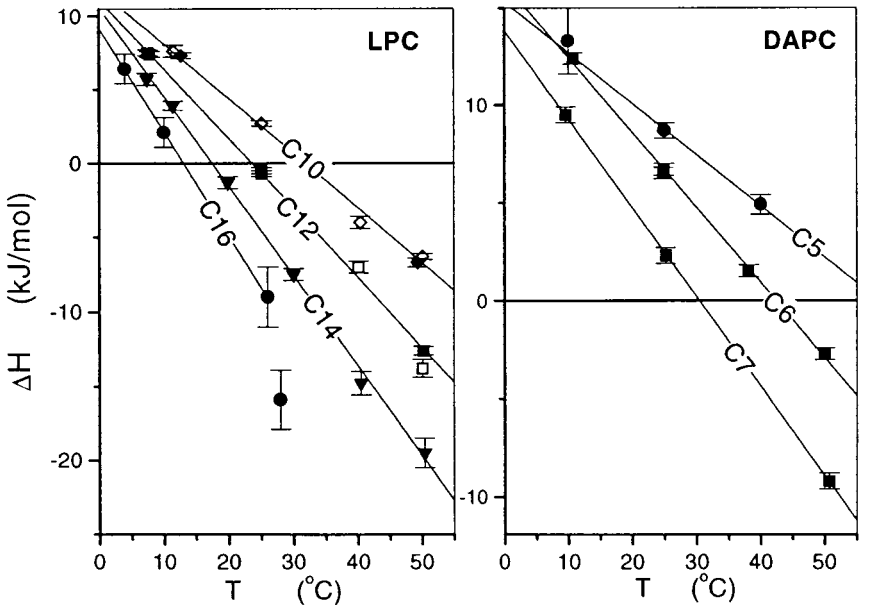

FIGURE 4 The heat of micelle formation for LPCs (*left*) and DAPCs (*right*) as a function of temperature. Experiments in water (*open symbols*) do not exhibit systematic differences from those in buffer. The slope of the linear fit lines yields ΔC_p.

Methylene group contributions

The standard free energy gain upon micelle formation, ΔG^0, is given by:

$$\Delta G^0 = RT \ln(\mathrm{CMC}/55.5\ \mathrm{M}) \qquad (3)$$

showing that ΔG^0 is related to the logarithm of the CMC. The incremental $\Delta\Delta G^0$ per methylene can be derived from the slope of the lines in Fig 4. Although chain length-dependent changes of the micellar geometry and, in turn, the headgroup interactions cannot strictly be ruled out, it is straightforward to assign the values of -3.1 ± 0.1 (LPC) and -2.5 ± 0.1 (DAPC) kJ/mol per methylene to the free energy changes upon transferring a methylene group from the initial monomer state to the state in which it is buried in the hydrophobic core of the micelle. These results are fairly compatible with literature data. An increment of -3.0 kJ/(mol) (~ -0.7 kcal/mol) has been reported for numerous hydrocarbons, alcohols, and one-chain amphiphiles (cf. Tanford, 1980; Clint, 1992 for reviews). The 20% lower effect per methylene of DAPCs agrees perfectly with Tanford's statement that their two chains "stick together" in water, covering 20% of the surface.

To study the consequences of the water-to-micelle transfer of methylene groups of DAPCs and LPCs, we have re-plotted the DAPC results as a function of the effective methylene number, n_{CH2}*(mon) (cf. Fig. 5). This quantity considers only methylene groups that are exposed to water (indicated by an asterisk) in the monomer state. Again, a methyl counts 1.5, so that n_{CH2}*(mon) = $0.8 \cdot n_{CH2}$ for DAPCs and n_{CH2}*(mon) = n_{CH2} for LPC.

The so-corrected methylene contributions to the free energy of LPCs and DAPCs (cf. Fig 5 *A*, now both -3.1 kJ/mol) agree with the literature value for hydrocarbons and

TABLE 2 Thermodynamic parameters of micelle formation

Compound	n_{CH2}	n_{CH2}*(mon)	CMC (25°C) (mM)	ΔC_p (J/(mol*K))	T* (°C)	ΔH (23°C)
C_{10}-LPC	9.5	9.5	6.8 ± 0.2	-370 ± 10	32	3.5 ± 0.6
C_{12}-LPC	11.5	11.5	0.71 ± 0.03	-470 ± 10	24	0.3 ± 0.5
C_{14}-LPC	13.5	13.5	0.045 ± 0.003‡	-600 ± 10	18	-3.2 ± 0.5
C_{16}-LPC†	15.5	15.5	0.005 ± 0.001	-690 ± 40	13	-7 ± 3
C_5-DAPC	9	7.2	90 ± 10	-260 ± 20	59	9 ± 1
C_6-DAPC	11	8.8	15 ± 1	-380 ± 10	43	7.6 ± 0.4
C_7-DAPC	13	10.4	1.9 ± 0.1	-460 ± 10	30	3.4 ± 0.1

The chain lengths of the compounds are specified in terms of the methylene number n_{CH2} (each methylene in the chains counts 1, methyl 1.5, carboxyl 0). The effective number of methylenes driving self-association considers only the part of the chain surface of a lipid monomer which is exposed to water, n_{CH2}*(mon). For LPCs, we find $n_{CH2} = n_{CH2}$*(mon) and for DAPCs, $n_{CH2} = 0.8 \cdot n_{CH2}$*(mon) due to an intramolecular interaction. The critical micelle concentrations, CMC, are displayed in Fig 3. Linear fits of ΔH vs. T (Fig 4., cf. Eq. 2, data weighted according to individual errors) yield as a slope the heat capacity change ΔC_p and, related to the intercept, the isocaloric temperature T* or ΔH at 23°C.

† For $T \leq 26$°C.

‡ At 20°C.

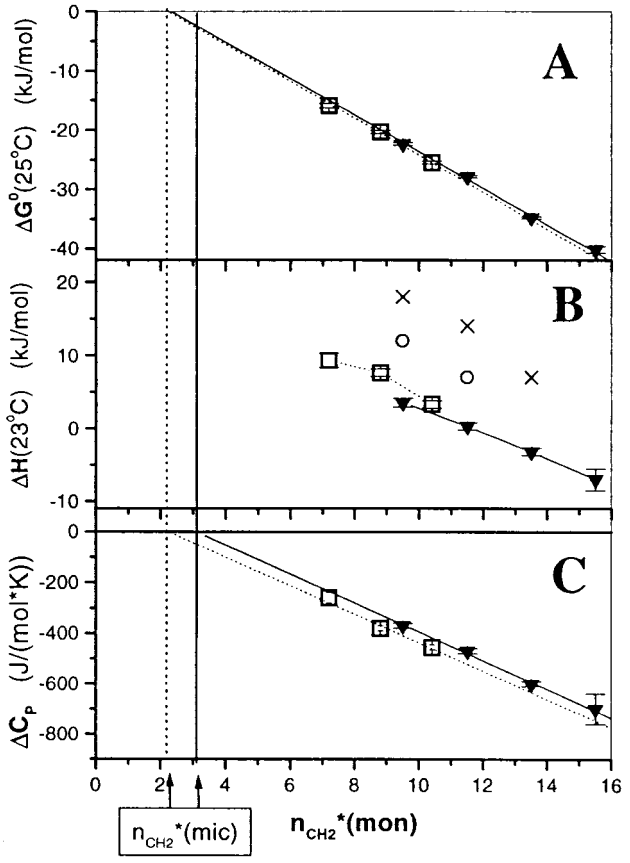

FIGURE 5 The standard free energy ΔG^0 (*A*), enthalpy ΔH at 23°C (*B*), and heat capacity change ΔC_p (*C*) of DAPCs (□) and LPCs (▼) of micelle formation versus the effective number of "driving" methylene groups (for explanation see text), n_{CH2}*(mon). ΔH of non-ionic detergents $C_{12}EO_7$ (×) and $C_{12}EO_3$ (○) (H. Heerklotz, unpublished data) at 25°C are shown for comparison. The vertical grid lines indicate the interface between water-accessible and buried methylenes as suggested by extrapolation to vanishing ΔC_p.

amphiphiles. The same applies to the incremental heat capacity changes, $\Delta\Delta C_p$, of -56 ± 9 (DAPCs) and -57 ± 3 (LPCs) J/(mol · K) per buried methylene (i.e., -28 and -28.5 J/(mol · K) per apolar hydrogen, respectively, cf. Fig 5 *C*) which is in accord with values between -28 and -33 J/(mol/K) per hydrogen reported for hydrocarbons, alcohols (see Tanford, 1980, for a review), or solid cyclic dipeptides (Murphy and Gill, 1991).

The incremental enthalpies per methylene at 23°C are of the order of $\Delta\Delta H$(23°C) ≈ -2 kJ/mol (Figs. 5 *B* and 6). According to $\Delta\Delta G^0 = \Delta\Delta H - T\Delta\Delta S$, we obtain each methylene contributing $\sim -T\Delta\Delta S \approx -1$ kJ/mol to the entropy of micelle formation, a value that is considerably smaller than the ~ -3 kJ/mol of liquid hydrocarbons.

DISCUSSION

Enthalpy of chain packing

We have shown that the methylene group contribution to the enthalpy of micelle formation at 23°C amounts to ~ -2 kJ/mol. This is quite different from the isocaloric solution (i.e., $\Delta\Delta H = 0$) of liquid hydrocarbons in water at this special temperature (Gill and Wadsö, 1976; Murphy et al., 1990; Baker and Murphy, 1998). This fact implies that a methylene group in a liquid crystalline micelle core has an enthalpic advantage of ~ -2 kJ/mol compared to one in a bulk oil, which is just compensated by a loss in entropy so that $\Delta\Delta G^0$ is not substantially affected.

Phillips et al. (1969) have compared the melting behavior of solid-like hydrocarbons and lipid bilayers in the gel phase, two states in which the chains are supposed to possess similar enthalpy and entropy. The solid-to-liquid transition of oils requires an enthalpy of ≈4 kJ/mol per methylene (Phillips et al., 1969; Lide, 1998) and the gel-to-liquid crystalline transition ≈2 kJ/mol per methylene (Phillips et al., 1969; Koynova and Caffrey, 1994), suggesting an enthalpy difference of ≈2 kJ/mol between liquid and liquid crystalline states at the respective melting temperatures. Phillips et al. (1969) have stressed that a direct comparison of enthalpies at markedly different temperatures is impossible for want of information about the heat capacity effects. The present study overcomes this problem because it refers to data at room temperature. The agreement between the incremental $\Delta\Delta H$ between liquid and liquid crystal obtained here and in the melting study (2 kJ/mol per methylene) implies that the effect is essentially independent of temperature, i.e., the corresponding incremental $\Delta\Delta C_p \approx 0$ (see below).

What accounts for the enthalpy and entropy differences between chain-chain interactions in solids/gels, liquid crystals, and liquids? The liquid crystalline-to-gel transition of lipid chains is accompanied by an increase in volume density by 3.5% (Nagle, 1973) and a stretching of the chains (all *trans*). Increased van der Waals interactions upon tighter packing and *gauche-trans* isomerization give rise to a gain in enthalpy ($\Delta\Delta H < 0$) but a loss in motional and conformational freedom ($\Delta\Delta S < 0$). Similar differences can be speculated to apply to liquid versus liquid crystalline structures. The important lesson from the observed chain-chain interaction characteristics is that it is by no means justified to approximate the enthalpic and entropic state of liquid crystalline chains by those in a bulk liquid.

Can we resolve systematic variations of the methylene group contributions $\Delta\Delta H$(23°C)? To answer this question, we have plotted them as a function of the effective chain length n_{CH2}*(mon) in Fig. 6 (derivative of traces in Fig. 5 *B*). For comparison, we have added previously unpublished data on a series of hepta and triethylene glycol alkyl ethers and values derived from literature data on sodium alkyl sulfates (Kresheck and Hargraves, 1974) and alkyldimethylphosphine oxides (Kresheck, 1998) (all taken at 25°C). At first glance we may stress that almost all incremental $\Delta\Delta H$ are in the range of -2 ± 1 kJ/mol as discussed above. It appears that the absolute value of the chain packing enthalpy tends to increase somewhat with increasing chain length. Note that lipid membranes exhibit order parameter profiles with a rather tightly packed "palisade layer" close to the surface and continuously decreasing order toward the

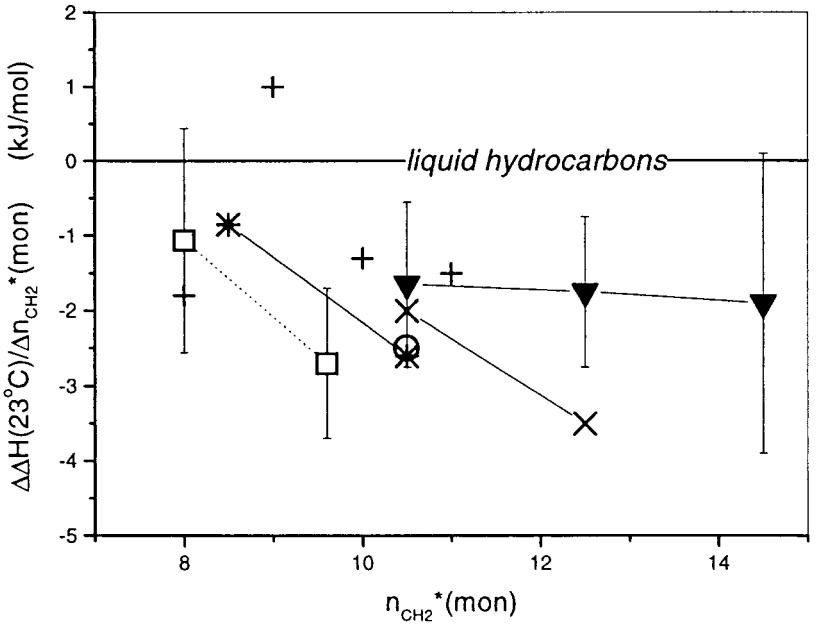

FIGURE 6 The methylene group contribution to ΔH of micelle formation at 23°C or 25°C as a function of the effective chain length, n_{CH2}*(mon). The data refer to the differences between the data for LPC (▼), DAPC (□), at 23°C and C_mEO_7 (×) and C_mEO_3 (○) shown in Fig 5 *B* and literature data for sodium alkyl sulfates (∗, Kresheck and Hargraves, 1974) and alkyldimethylphosphine oxides (+, Kresheck, 1998) at 25°C. The effect of the slightly different reference temperatures (23 vs. 25°C) on $\Delta\Delta H$ is negligible (≈ -0.1 kJ/mol).

chain end (Seelig and Seelig, 1980). Similarly, larger cores of micelles could result in increasing mean order. Furthermore, it seems that packing improvements by reducing the size of the headgroup (C_mEO_7 to C_mEO_3) or by adding a second chain per headgroup (LPCs to DAPCs) also make $\Delta\Delta H$ somewhat more exothermic. However, more and more accurate data will be required to provide additional evidence for these suggestions. We should note that the difference between LPC and DAPC is related to the implicit assumption that the intramolecular chain/chain interactions do not change their interaction enthalpy upon micelle formation, a plot versus n_{CH2} instead of n_{CH2}*(mon) yields methylene increments similar to those of LPC.

The interactions discussed above are of major importance for the thermodynamics of the incorporation of hydrophobic or amphiphilic molecules into lipid membranes. Let us first consider the incorporation of surfactants into lipid bilayers resulting in the disturbance of acyl chain packing by creating a (positive) curvature strain. As a consequence, each surfactant reduces the order of a number of neighboring lipid molecules. The enthalpies of incorporation are, indeed, endothermic at room temperature (Heerklotz and Seelig, 2000b) in the absence of specific interactions (Malloy and Binford, 1990). The disordering effect on the lipids could also account for the fact that the transfer of surfactants from micelles into bilayers is also, mostly, endothermic (Heerklotz et al., 1998). Exceptions are the incorporation of lysolecithin into vesicles of MeDOPE (Epand and Epand, 1994) or that of the detergent $C_{12}EO_3$ into POPC vesicles (Heerklotz et al., 1998). In both cases, the packing of the chains in the membrane is suggested to be improved upon solute insertion because either the host lipid (MeDOPE) or the solute ($C_{12}EO_3$) exhibits a negative intrinsic curvature so that strains are released in the host-guest mixture. The complex packing effects in lipid/surfactant mixed membranes can give rise to nonlinear relationships between enthalpy and chain length (Heerklotz and Seelig, 2000a) and anomalous heat capacity changes.

Other examples of ordering/disordering effects of the chains show similar enthalpy characteristics. The heat of incorporation of a solute into small lipid vesicles (SUV) is often much less endothermic (or even exothermic) compared with the partitioning into large vesicles (LUV). This phenomenon has been observed by Seelig and co-workers and established as the nonclassical hydrophobic effect (Seelig and Ganz, 1991; Seelig, 1997). For example, the heat of binding of magainin 2 amide to LUV is ~23 kJ/mol more endothermic than into SUV (Wieprecht et al., 2000). Again, the effect is almost completely compensated by a loss of entropy and may be explained in terms of the poorer acyl chain packing in SUV that becomes less disturbed or even improved upon intercalation of a solute than in the case of LUV. Finally, Nebel et al. (1997) have measured that the (chain disordering) osmotic inflation of vesicles is endothermic, whereas osmotic compression is exothermic.

Apparent water-accessible apolar surface

It has been shown that the heat capacity change ΔC_p can be empirically related to changes in hydrophobic and hydrophilic solvation (for a review see Baker and Murphy, 1998). Because the headgroups remain hydrated upon micelle formation, ΔC_p can be assumed to solely reflect changes in the exposure of hydrophobic groups to water (Kresheck and Hargraves, 1974; Paula et al., 1995). The ΔC_p values of LPCs can be interpreted as the sum of the group contributions (-57 J/(mol · K)) from all but n_{CH2}*(mic) $\approx$ 3.1

methylenes. Note that this value can be directly read from Fig. 5 *C* as the intercept of the fit lines with the abscissa. A smaller value of 2.2 methylenes is suggested for DAPCs, but the difference is not strictly significant considering an uncertainty of $\sim\pm1$ CH_2. Taking into account a water-accessible surface increment of 31 $Å^2$ per methylene (De Young and Dill, 1988), we can calculate the apparent water-accessible apolar surface area, ASA_{ap}, according to n_{CH2}*(mic) · 31 $Å^2$ or, equivalently, to ΔC_p/1.84 J/(mol · K · $Å^2$). The results are of the order of 70 (DAPCs) and 100 (LPCs) $Å^2$.

It is by no means straightforward to relate the apparent ASA_{ap} to structural parameters such as the smooth geometric lateral area increment per lipid, A_0, which amounts to $\sim$60 $Å^2$ for the DAPCs studied here (Eastoe et al., 1998; Tausk et al., 1974) and to similar values for membrane lipids (cf., e.g., Nagle et al., 1996; Nagle and Tristam-Nagle, 2000). On one hand, the roughness of the interface, which is structurally described as an overlap of hydrocarbon and water domains by $\sim$5–8 $Å^2$ (Wiener and White, 1992), will increase ASA_{ap} compared to A_0. On the other hand, the surface is covered by headgroups that not only reduce the water accessibility of the interface, but also greatly affect the dynamic and structural properties of the interfacial water molecules which are, after all, responsible for ΔC_p. The apparent ASA_{ap} must thus be considered the oil/water interface, which would have the same free energy as the chain/water interface of the micelle, $\sim$9 kJ/mol LPC.

The real rough interface would, in fact, be larger than the apparent ASA_{ap} if the contact of the chains to bound water was energetically "cheaper" than to bulk water. A solution of the problem might be possible by molecular dynamics simulations, which allow access of both structural and thermodynamic parameters simultaneously.

Apparent interactions of the water accessible regions

Above, we have argued that each of the n_{CH2}*(mon)-n_{CH2}*(mic) methylene groups, which are transferred from an aqueous to an apolar environment, contributes -3.1 kJ/mol to ΔG^0. This contribution vanishes if we extrapolate ΔG^0 vs. n_{CH2}*(mon) toward n_{CH2}*(mic), as illustrated by fit and grid lines in Fig. 5, *A* and *B*. Then, the "remaining" small $\Delta G^0(n_{CH2}$*(mic)) of 0 ± 1 (DAPCs) and -2 ± 1 (LPCs) can be interpreted as the sum of the interactions between the water-exposed moieties. That means that all other interactions, except hydrophobic forces, between the lipids essentially compensate each other and the overall ΔG^0 represents almost exclusively hydrophobic interactions.

When it comes to the enthalpic effects, it is not as straightforward to perform a linear extrapolation because the packing properties of methylene groups may vary between different positions. It may, however, be supposed that the tendencies are, at least, monotonic. Consequently, enthalpic interactions between the water-accessible moieties of the order of 10–20 kJ/mol are suggested. These interactions are, obviously, compensated by entropy gains because ΔG^0 is essentially unaffected (see above).

We conclude that the rather small enthalpies of micelle formation measured at room temperature must not be interpreted in terms of headgroup interactions. They reflect a balance between substantially endothermic headgroup interactions and exothermic chain packing effects.

CONCLUSIONS

The self-association of phospholipids is almost exclusively controlled by hydrophobic, i.e., chain/water interactions. The incremental standard Gibbs free energy $\Delta\Delta G^0 = -3.1$ kJ/mol and heat capacity $\Delta\Delta C_p = -57$ J/(mol · K) per methylene group do not depend on whether it is buried in bulk oil or in the core of a micelle. The two-chain surfactants yield these values after correction for an intramolecular interaction covering 20% of the chain surface. The heat capacity changes can be interpreted as the sum of the group contributions from all but three methylenes per LPC. In other words, about three methylene groups per lipid remain, on the average, exposed to water so that potential hydrophobic interactions of ~-9 kJ/mol cannot be realized. This fact is described by an apparent water-accessible apolar surface area $ASA_{ap} \approx 100$ $Å^2$. Further studies are required to prove the suggestion that the aggregates of two-chain compounds are more stable (interfacial $\Delta G^0 \approx 6$ kJ/mol, two methylenes, 70 $Å^2$).

When it comes to the enthalpy and entropy of the chain/chain interactions, the liquid crystalline state differs considerably from bulk oil. The partial alignment of the liquid-crystalline chains improves the enthalpy of the chain-chain interaction by $\Delta\Delta H$ of ~-2 kJ/mol per methylene. $\Delta\Delta H$ is quantitatively compensated by an accompanying loss of conformational and/or motional entropy. This effect is supposed to control the enthalpy of insertion of compounds into lipid membranes at room temperature.

The water-exposed regions ("headgroup interactions") yield almost no contribution to the free energy of micelle formation, but give rise to a substantial endothermic interaction enthalpy.

H.H.H. thanks the German Academic Exchange Service (DAAD) for a fellowship. We acknowledge support from the Medical Research Council of Canada and are indebted to MicroCal Inc. for the opportunity to perform ITC experiments at the company laboratory. We are grateful to Drs. J. Seelig, H. Binder, T. Wieprecht, S. Feller, and D. Lichtenberg for important comments.

REFERENCES

Baker, B. M., and K. P. Murphy. 1998. Prediction of binding energetics from structure using empirical parametrization. *Methods Enzymol.* 295: 294–314.

Blume, A. 1983. Apparent molar heat capacities of phospholipids in aqueous dispersion. Effects of chain length and head group structure. *Biochemistry.* 22:5436–5442.

Chernomordik, L. 1996. Non-bilayer lipids and biological fusion intermediates. *Chem. Phys. Lipids.* 81:203–213.

Clint, J. H. 1992. Surfactant Aggregation. Blackie & Son, Glasgow.

DeVido, D. R., J. G. Dorsey, H. S. Chan, and K. A. Dill. 1998. Oil/water partitioning has a different thermodynamic signature when the oil solvent chains are aligned than when they are amorphous. *J. Phys. Chem. B.* 102:7272–7279.

De Young, L. R., and K. A. Dill. 1988. Solute partitioning into lipid bilayer membranes. *Biochemistry.* 27:5281–5289.

Eastoe, J., J. S. Dalton, and R. K. Heenan. 1998. Dynamic surface tensions and micelle structures of dichained phosphatidylcholine surfactant solutions. *Langmuir.* 14:5719–5724.

Epand, R. M., and R. F. Epand. 1994. Calorimetric detection of curvature strain in phospholipid bilayers. *Biophys. J.* 66:1450–1456.

Gill, S. J., and I. Wadsö. 1976. An equation of state describing hydrophobic interactions. *Proc. Natl. Acad. Sci. USA.* 73:2955–2958.

Heerklotz, H. H., H. Binder, and H. Schmiedel. 1998. Excess enthalpies of mixing in phospholipid-additive membranes. *J. Phys. Chem. B.* 102: 5363–5368.

Heerklotz, H., G. Lantzsch, H. Binder, G. Klose, and A. Blume. 1996. Thermodynamic characterization of dilute aqueous lipid/detergent mixtures of POPC and C12EO8 by means of isothermal titration calorimetry. *J. Phys. Chem.* 100:6764–6774.

Heerklotz, H., and J. Seelig. 2000a. Correlation of the membrane/water partition coefficients of detergents with the critical micelle concentration. *Biophys. J.* 78:2435–2440.

Heerklotz, H., and J. Seelig. 2000b. Titration calorimetry of surfactant-membrane partitioning and membrane solubilization. *Biochim. Biophys. Acta.* 1508:69–85.

Huster, D., K. Arnold, and K. Gawrisch. 1999. Investigation of lipid organization in biological membranes by two-dimensional nuclear Overhauser enhancement spectroscopy. *J. Phys. Chem. B.* 103:243–251.

Israelachvili, J., and H. Wennerstrom. 1996. Role of hydration and water structure in biological and colloidal interactions. *Nature.* 379:219–225.

Kessi, J., J. C. Poiree, E. Wehrli, R. Bachofen, G. Semenza, and H. Hauser. 1994. Short-chain phosphatidylcholines as superior detergents in solubilizing membrane proteins and preserving biological activity. *Biochemistry.* 33:10825–10836.

Killian, J. A. 1998. Hydrophobic mismatch between proteins and lipids in membranes. *Biochim. Biophys. Acta.* 1376:401–415.

Kluge, S., K. Gawrisch, and P. Nuhn. 1987. Loss of infectivity of red clover mottle virus by lysolecithin. *Acta Virol.* 31:185–188.

Koynova, R., and M. Caffrey. 1994. Phases and phase transitions of the glycoglycerolipids. *Chem. Phys. Lipids.* 69:181–207.

Kresheck, G. C. 1998. A calorimetric determination of the standard enthalpy and heat capacity changes that accompany micelle formation for four long chain alkyldimethylphosphine oxides in H_2O and D_2O solution from 15 to 79°C. *J. Am. Chem. Soc.* 120:10964–10969.

Kresheck, G. C., and W. A. Hargraves. 1974. Thermometric titration studies of the effect of headgroup, chain length, solvent, and temperature on the thermodynamics of micelle formation. *J. Colloid Interface Sci.* 48:481–493.

Lide, D. R. 1998. CRC Handbook of Chemistry and Physics. CRC Press, Boca Raton.

Ludtke, S., K. He, and H. Huang. 1995. Membrane thinning caused by magainin 2. *Biochemistry.* 34:16764–16769.

Malloy, R. C., and J. S. Binford. 1990. Enthalpy titration and solubilization of dimyristoylphosphatidylcholine vesicles with bile salts. *J. Phys. Chem.* 94:337–345.

Murphy, K. P., and S. J. Gill. 1991. Solid model compounds and the thermodynamics of protein unfolding. *J. Mol. Biol.* 222:699–709.

Murphy, K. P., P. L. Privalov, and S. J. Gill. 1990. Common features of protein unfolding and dissolution of hydrophobic compounds. *Science.* 247:559–561.

Nagle, J. F. 1973. Lipid bilayer phase transition: density measurements and theory. *Proc. Natl. Acad. Sci. USA.* 70:3443–3444.

Nagle, J. F., and S. Tristam-Nagle. 2000. Structure of lipid bilayers. *Biochim. Biophys. Acta.* 1469:159–195.

Nagle, J. F., R. Zhang, S. Tristram-Nagle, W. Sun, H. I. Petrache, and R. M. Suter. 1996. X-ray structure determination of fully hydrated L alpha phase dipalmitoylphosphatidylcholine bilayers. *Biophys. J.* 70: 1419–1431.

Nebel, S., P. Ganz, and J. Seelig. 1997. Heat changes in lipid membranes under sudden osmotic stress. *Biochemistry.* 36:2853–2859.

Olofsson, G. 1985. Microtitration calorimetric study of the micellization of three poly(oxyethylene) glycol dodecyl ethers. *J. Phys. Chem.* 89: 1473–1477.

Paula, S., W. Süs, J. Tuchtenhagen, and A. Blume. 1995. Thermodynamics of micelle formation as a function of temperature: a high sensitivity titration calorimetry study. *J. Phys. Chem.* 99:11742–11751.

Phillips, M. C., R. M. Williams, and D. Chapman. 1969. On the nature of hydrocarbon chain motions in liquid crystals. *Chem. Phys. Lipids.* 3:234–244.

Sanders, C. R., and G. C. Landis. 1995. Reconstitution of membrane proteins into lipid-rich bilayered mixed micelles for NMR studies. *Biochemistry.* 34:4030–4040.

Seelig, J. 1997. Titration calorimetry of lipid-peptide interactions. *Biochim. Biophys. Acta.* 1331:103–116.

Seelig, J., and P. Ganz. 1991. Non-classical hydrophobic effect in membrane binding equilibria. *Biochemistry.* 30:9354–9359.

Seelig, J., and A. Seelig. 1980. Lipid conformation in model membranes and biological membranes. *Q. Rev. Biophys.* 13:19–61.

Sharp, K., and B. Madan. 1997. Hydrophobic effect, water structure, and heat capacity changes. *J. Phys. Chem. B.* 101:4343–4348.

Spolar, R. S., J. R. Livingstone, and M. T. Record, Jr. 1992. Use of liquid hydrocarbon and amide transfer data to estimate contributions to thermodynamic functions of protein folding from the removal of nonpolar and polar surface from water. *Biochemistry.* 31:3947–3955.

Tanford, C. 1980. The hydrophobic effect: formation of micelles and biological membranes. John Wiley & Sons, New York.

Tausk, R. J. M., J. Karmiggelt, C. Oudshoorn, and J. T. G. Overbeek. 1974. Physical chemical studies of short-chain lecithin homologues. I. Influence of the chain length of the fatty acid ester and of electrolytes on the critical micelle concentration. *Biophys. Chem.* 1:175–183.

Vold, R. R., and R. S. Prosser. 1996. Magnetically oriented phospholipid bilayered micelles for structural studies of polypeptides. Does the ideal bicelle exist? *Cryobiology.* 113:267–271.

Wiener, M. C., and S. H. White. 1992. Structure of a fluid dioleoylphosphatidylcholine bilayer determined by joint refinement of x-ray and neutron diffraction data. III. Complete structure. *Biophys. J.* 61: 437–447.

Wieprecht, T., O. Apostolov, and J. Seelig. 2000. Binding of the antibacterial peptide magainin 2 amide to small and large unilamellar vesicles. *Biophys. Chem.* 85:187–198.

Yuan, Y., S. M. Schoenwaelder, H. H. Salem, and S. P. Jackson. 1996. The bioactive phospholipid, lysophosphatidylcholine, induces cellular effects via G-protein-dependent activation of adenylyl cyclase. *J. Biol. Chem.* 271:27090–27098.